OPTIMIZATION OF THE NORMAL METAL HOT-ELECTRON MICROBOLOMETER

D. Chouvaev, D. Golubev, M. Tarasov*, and L. Kuzmin

Department of Microelectronics and Nanoscience,
Chalmers University of Technology, SE-412 96 Gothenburg, Sweden

**Inst. of Radioengineering and Electronics RAS, Mokhovaya 11, 103907 Moscow, Russia*

Abstract

The purpose of our project is to create a robust fully on-chip integrated antenna-coupled bolometer, competitive in sensitivity for radio-astronomy applications. It must have noise equivalent power (NEP) below 10^{-17} W/Hz$^{1/2}$ and time constant shorter then 1 ms. We call this device a normal metal hot-electron microbolometer (NHEB), because its function is based on the hot-electron effect in a strip of a normal metal at temperatures below 0.5 K.

Until now we have been developing the power sensor for this device. In the beginning we could not operate the sensor at electronic temperatures below 300 mK, presumably because of the high external noise load. Our latest results show how this problem can be solved experimentally. We have achieved noise performance mostly limited by the amplifier, which corresponds to expected detector NEP on the order of $1.5 \cdot 10^{-17}$ W/Hz$^{1/2}$ at 100 mK.

We have also performed a theoretical analysis of temperature readout by NIS tunnel junctions in our device. In particular heat flow fluctuations are discussed as an additional noise component, which needs to be included in the analysis. Our model allows us to calculate optimal ranges of parameters like normal resistance of the junction or optimal bias current, to provide the lowest NEP for given operating conditions (temperature, phonon noise etc.).

1. Introduction

Bolometers are direct broad band detectors of electromagnetic radiation, complementing heterodyne detectors in radio-astronomy research. They are useful, for example, for investigating the cosmic microwave background. Most common bolometers used in radio-astronomy are made with a suspended absorber, being heated by incident radiation, and a semiconducting thermistor. Cooled to 100 mK, they can provide sensitivity better then $3 \cdot 10^{-17}$ W/Hz$^{1/2}$ with time constant down to 10 ms [1]. An alternative to those are superconducting bolometers, where the sensor is a suspended chip with a superconducting

structure. Being kept by electrothermal feedback at the superconducting transition, this system reacts strongly on signal-induced temperature variations around T_c (≈300 mK) [2].

One disadvantage with the existing bolometers is that they compromise sensitivity and speed – to reach NEP < 10^{-17} W/Hz$^{1/2}$ one needs to make the absorbing area large, thus getting also large thermal capacity and, consequently, longer reaction time. The thermal reaction time is defined as $\tau=C/G$, where C is the absorber's thermal capacity and G is thermal conductance from the absorber to the environment.

Another problem is that suspended structures are often fragile, and it is difficult to combine many of them into a 2D detector array. Building a fully planar-integrated 2D array of detectors with sensitivity better then 10^{-17} W/Hz$^{1/2}$ and time constant under 1 ms can be regarded as a challenge in bolometer research.

The device proposed in [3] and later partly implemented [4] can be a promising choice. This is a planar microfabricated bolometer, using an antenna (which can be integrated on the same chip) to receive a signal. The schematic picture of the whole circuit and an SEM-image of a fabricated sensor can be seen in fig. 1. In an antenna-coupled bolometer there is no need to make the sensor itself large to receive more power, instead it can be miniaturized, minimizing also the thermal capacity.

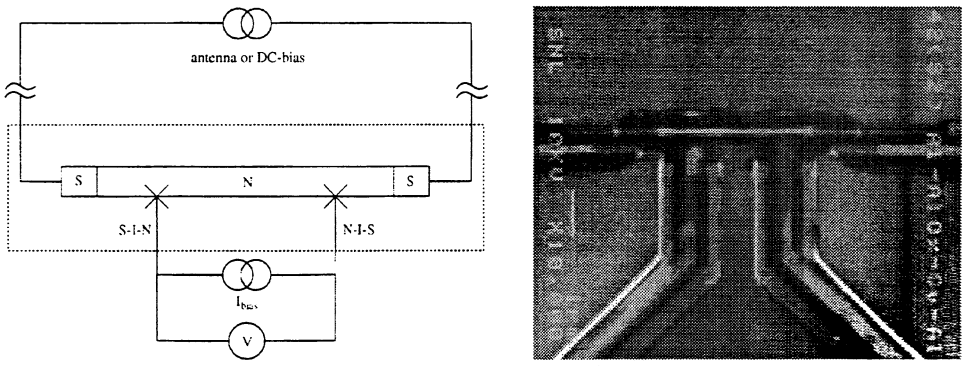

FIG. 1. The original device scheme and an SEM-image of a real sample. Double NIS tunnel junctions are used to increase the response dV/dT and to simplify biasing.

A microwave signal received by the antenna will induce current in a normal-metal resistor (further referred to as "absorber"), this current will dissipate and generate Joule heat. This heat, however, will be delivered not to the whole structure at once, but first to the electron gas in the resistor. At temperatures below 0.5 K, where ultra-sensitive bolometers are operated, the thermal coupling between electrons and phonons is very low, and the electrons will establish their own equilibrium at a temperature above the phonon temperature in the surrounding body (hot electron effect). In this sense, the electron gas in the resistor can be seen as a power absorber, and the thermal conductance to the

environment is then limited by the energy exchange rate between the electrons and the phonons. Thus one does not need to suspend the absorber to thermally isolate it. Furthermore, the thermal capacity of the electrons is much less than the thermal capacity of the whole structure, and this makes the sensor very fast.

The only problem left is that the heated electrons could diffuse back to the antenna instead of exchanging energy with phonons in the resistor. Fortunately this can be avoided by making the antenna superconducting, since a property of a superconductor-normal metal interface is that electric current passes it without transferring the thermal energy of electrons (Andreev reflection).

Finally, very small signal power results in a substantial rise of the electron temperature in the absorber. These temperature variations need to be converted to some electrical response, and this is accomplished using one or two normal-metal/insulator/ superconductor (NIS) tunnel junctions, where the normal electrode is the absorber. Their IV-characteristics get broadened with increasing electron temperature in the N-electrode. When such a junction (or a pair of those) is biased with constant current in the sub-gap region, the voltage over the junction will depend on the thermal smearing, and it will be proportional to the electron temperature in a wide range (fig. 2).

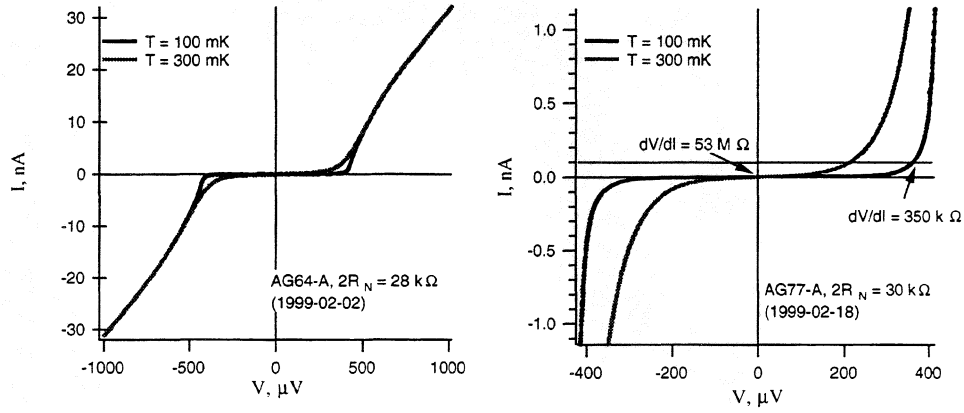

FIG. 2. Principle of measuring electron temperature by means of an NIS or SINIS tunnel junction stucture biased with constant current.

The power responsivity of this sensor is a ratio of two terms: temperature responsivity (dV/dT) and heat conductance from the electrons to the environment ($G = dP/dT$):

$$S = \frac{dV}{dP} = \left|\frac{dV}{dT}\right| \cdot \left|\frac{dP}{dT}\right|^{-1}$$

The temperature responsivity depends on properties of the tunnel junctions and it is nearly constant almost in the whole range of operating temperatures (typically $dV/dT \approx 5\text{-}10 \cdot 10^{-4}$ V/K). The heat conductance depends mostly on properties of the absorber and can be estimated from the ideal energy exchange rate between electrons and phonons in equilibrium at different temperatures:

$$P = \Sigma\Omega(T_e^5 - T_p^5) \quad \rightarrow \quad \frac{dP}{dT} = 5\Sigma\Omega T_e^4 ,$$

where Ω here is the absorber volume and Σ is a specific material parameter. For realistic device parameters (namely for our sample AG77) this gives power responsivity

$$S = \frac{1}{T_e^4} 8 \cdot 10^5 \, {}^{VK^4}\!/_{W} \quad \rightarrow \quad S(0.3\text{K}) = 1 \cdot 10^8 \, {}^{V}\!/_{W} , \quad S(0.1\text{K}) = 3 \cdot 10^9 \, {}^{V}\!/_{W} .$$

Accordingly, a decrease of the operating temperature has great advantages, limited though by the fact that dV/dT rapidly falls below 100 mK. Knowing the power responsivity, we can also estimate the noise equivalent power (NEP) of the detector. Assuming that the total noise is dominated by amplifier noise, and that we use a very good amplifier ($\sqrt{S_V} = 3\text{nV/Hz}^{1/2}$) we get

$$NEP(0.3\text{K}) = 3 \cdot 10^{-17} \, {}^{W}\!/_{\sqrt{Hz}} , \quad NEP(0.1\text{K}) = 1 \cdot 10^{-18} \, {}^{W}\!/_{\sqrt{Hz}} ,$$

which is superior to most of the existing devices.

The thermal reaction time will be determined by the electron-phonon interaction time, estimated to

$$\tau \approx 2 \cdot 10^{-8} \cdot T_e^{-3} \text{sK}^3 \quad \rightarrow \quad \tau(0.3\text{K}) = 0.8\mu\text{s} , \quad \tau(0.1\text{K}) = 20\mu\text{s} .$$

This is also well below of what is usually required (1 ms).

2. Device fabrication and measurement setup

The power sensor ("microcalorimeter") is fabricated by e-beam lithography and shadow metal evaporation. Three metal layers are used – a superconductor for NIS tunnel junctions (aluminum film, 36-38 nm), a normal metal for the power absorber (copper, 58 nm), and one more superconducting layer for the absorber bias leads or eventually the antenna (aluminum, 70 nm). The tunnel junctions are formed by oxidizing the first superconducting layer before deposition of the normal metal on top of it. Typical oxidation conditions are $P(O_2)$ = 0.3-0.4 mbar and t = 0.5-2 min, this results in the junction normal resistance of 5-15 kΩ for area about 0.1 μm^2. The tricky part is to contact the same absorber strip both by an oxidized superconductor (NIS junctions) and by a superconductor with a very transparent interface to the normal metal (absorber bias electrodes). This can be done either by a two-step process with two

lithography/deposition steps and ion beam cleaning in-between, or by our new single-step process where tilting of a sample in two perpendicular planes is employed (fig. 3).

The dimensions of the absorber in the most recent modification of our device are $4.5 \times 0.25\ \mu m^2$, thickness 58 nm, copper. Its resistance is about 20 Ω, which is not optimal for matching to an antenna. That is why we are planning to decrease the width to 0.1 μm and increase the length in the future. Changing the absorber material to chromium is another option.

For dc-measurements we have used a current bias to introduce heat into the absorber instead of connecting any antenna. The measurements are done in a dilution refrigerator capable of cooling samples to 25 mK. There is no possibility to irradiate a sample with sub-mm-waves in this cryostat. The current source for the NIS junctions' bias (and the same kind for the absorber bias) is made up of a symmetric voltage source and two high-value (10 or 100 MΩ) resistors in series (at room temperature). Johnson noise in those resistors is the main source of bias noise discussed in part 4.

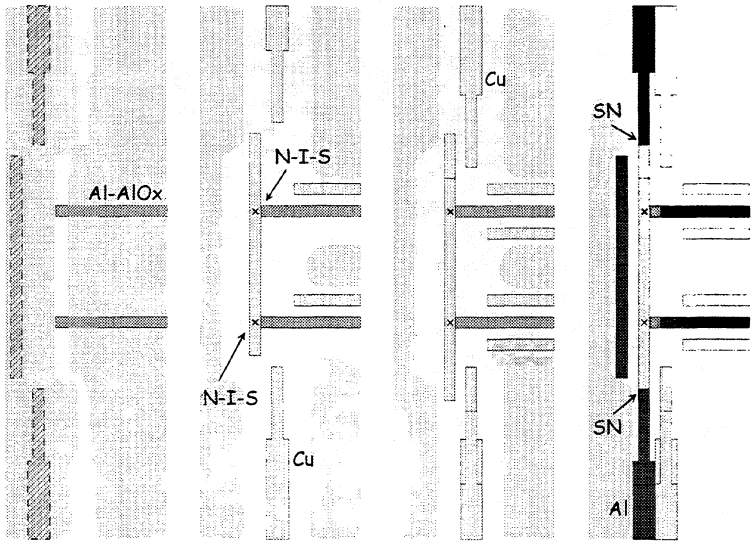

FIG. 3. Schematic picture of the metal deposition process. A double PMMA-copolymer resist is used to make a suspended mask. In the leftmost picture both resist layers are shown by slightly darker areas, on the three others – only the underlying copolymer mask. By tilting the sample in different planes the metal structures are shifted in respect to the original openings in the PMMA-mask, providing also necessary overlaps between subsequently deposited metal layers.

The measurements include a calibration measurement, where the voltage response from the tunnel junctions at the working bias is studied as a function of temperature in the cryostat without applying any additional heating to the absorber. IV-curves of the tunnel junctions at different cryostat temperatures are registered to determine or verify the choice of the working point, as well as for diagnostics of the junction quality. Then we can test the sensor by driving current through the absorber and measuring the response at a fixed cryostat temperature. Finally, noise spectra at different measurement conditions can be taken.

3. Experimental results

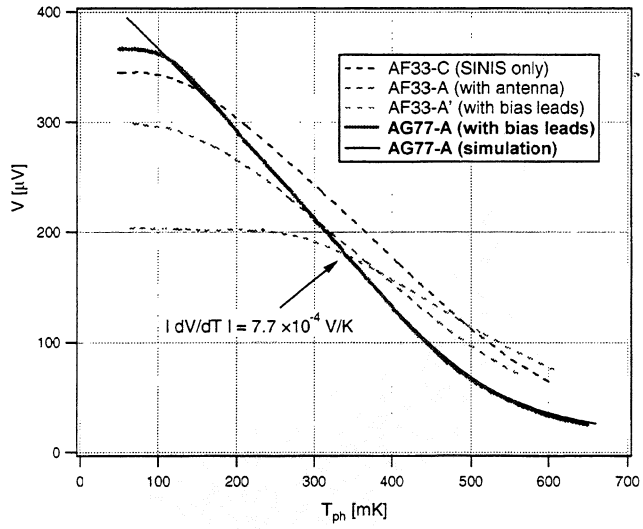

FIG. 4. Comparison of V(T) dependencies for different structures on sample AF33 (older data – dashed curves) and the same dependence for sample AG77, where additional tunnel junctions in the absorber bias circuit have been used (the thick curve). A strong saturation can be seen for the structure with long bias leads on the sample AF33. Saturation is present even for the sample AG77, but only below 100 mK. The thin curve is a theoretical fit for this sample's V(T).

When we started our experiments, we obtained good power responsivity (at the predicted level) at relatively high electron temperatures above 300 mK. However, at first we did not manage to obtain any good results where they were most expected – in the temperature range 100-300 mK. The reason for this was saturation of the response V(T) of the tunnel junctions, apparently seen in the calibration curves (fig. 4). Yet worse, the measured noise level used to be an order of magnitude higher then the noise of our amplifier, which had

modest 30 nV/Hz$^{1/2}$ at 10 Hz. It has taken a while to realize that those phenomena must have had the same cause, namely an intensive and noisy input signal, coupling to the absorber and heating the electrons sometimes above +300 mK. Two clues convinced us of the validity of this hypothesis: a comparison of noise and gain (=power responsivity) of the device (fig. 5a) and the dependence $T_{electron}(T_{phonon})$ of the absorber where $T_{electron}$ had been deduced by fitting IV-curves of the tunnel junctions at different temperatures (fig. 5b).

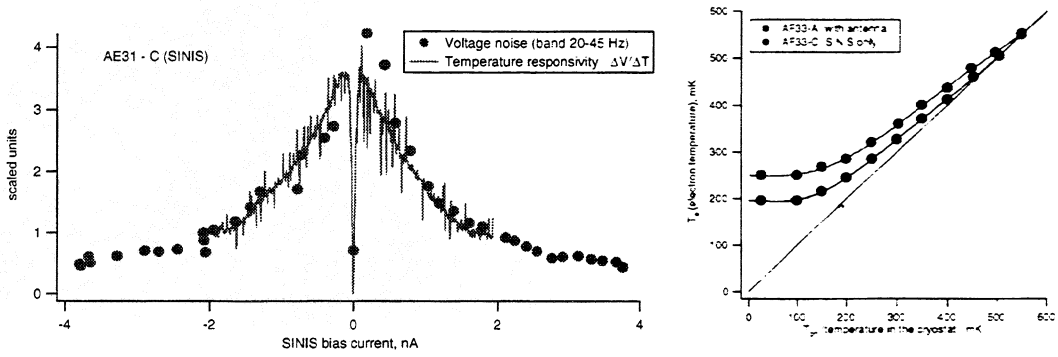

a) b)

FIG. 5. a) Spot noise and dV/dT plotted on the same graph for one of the older samples: both dependencies have very similar shapes, which must indicate that the noise is present already as fluctuations of electron temperature in the absorber, i.e. at the input. b) $T_{electron}$ (deduced from fits of IV-curves for SINIS double junctions) vs. temperature T_{ph} at which those IV-curves have been taken; data for sample AF33 (see also fig. 4).

Once being convinced about the presence of external heating we tried to identify how the noise comes in. Pick-up in the circuit connected for heating the absorber was one suggestion, a microwave "leakage" into the sample cavity was another one. Eliminating the second being a more difficult task, we started by breaking the absorber bias circuit by high-resistive elements close to the absorber. We hoped that the voltage induced in that low-ohmic (R_{abs} = 20 Ω) circuit by microphonics will drop on those high-resistive links, thus not being able to generate any noticeable current. We have chosen NIS tunnel junctions on both sides of the absorber as such protecting links, since they have very high intrinsic resistance in the sub-gap region, and they are very easy to fabricate (fig. 6).

This measure has given surprisingly good results, bringing the V(T) saturation down to 100-130 mK (fig. 4), and the noise level almost to the amplifier level. However, if we look at the noise spectra (fig. 7), we may notice, that connecting wires to the absorber and closing this circuit result in additional noise contributions, thus indicating that even this strong protection is not perfect. Furthermore, even the noise associated with an isolated

"absorber" island (7-10 $nV/Hz^{1/2}$) is clearly higher then what is expected from the thermometry noise (3 $nV/Hz^{1/2}$). We think that some high-frequency leak still exists and that it is responsible for this additional noise. Re-calculated to NEP the measured voltage noise corresponds to about $1.5 \cdot 10^{-17}$ $W/Hz^{1/2}$ at 10 Hz.

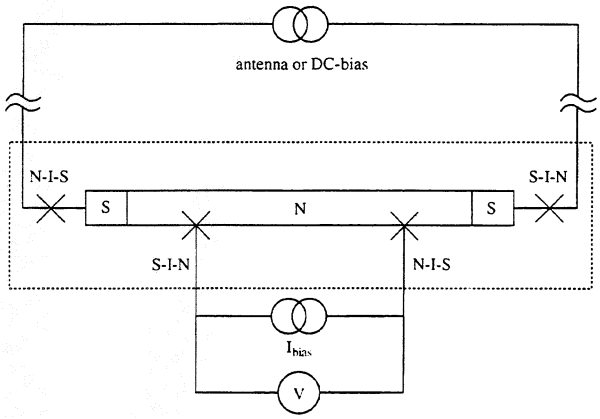

FIG. 6. The modified structure with additional NIS tunnel junctions in the absorber bias circuit.

However, the protection by tunnel junctions distorted completely the heating power calibration at $I_{absorber} > 0$. Earlier we could assume that the dissipated power was $P=P_J=R_{absorber} \times I^2_{absorber}$. Now, as soon as $I_{bias}>0$ high-energy electrons are injected into the superconducting electrode of the protecting NIS-junction, and further to the absorber, where this energy apparently dissipates, giving $P>>P_J$. This effect is similar to the electronic cooling by NIS tunnel junctions described elsewhere [5], but now our object is on the "warm" side of the Peltier cooler. This is the reason why we still can not report the calibrated experimental value of the power responsivity of our device at low temperature (100 mK).

This unfortunate situation does not seem to be a real obstacle. Simply reversing the NIS junctions and thus setting the N-part at the absorber side should be enough to solve the problem. An additional NS-interface between the superconducting electrodes going to the absorber and the N-side of the protecting junctions would interrupt the unwanted energy flow due to the Andreev reflection. Another simple (but probably not as elegant) solution is to use small external resistors, which can be bonded to the chip wiring, instead of tunnel junctions as high-resistive links.

Whatever difficulties can be expected in characterizing the device by applying a dc-current, the new results show that there are no severe problems with the sensor itself. If

we manage to couple the absorber efficiently to an integrated antenna, and place the device in an enclosure with well-controlled input of high-frequency radiation, we expect it to function properly.

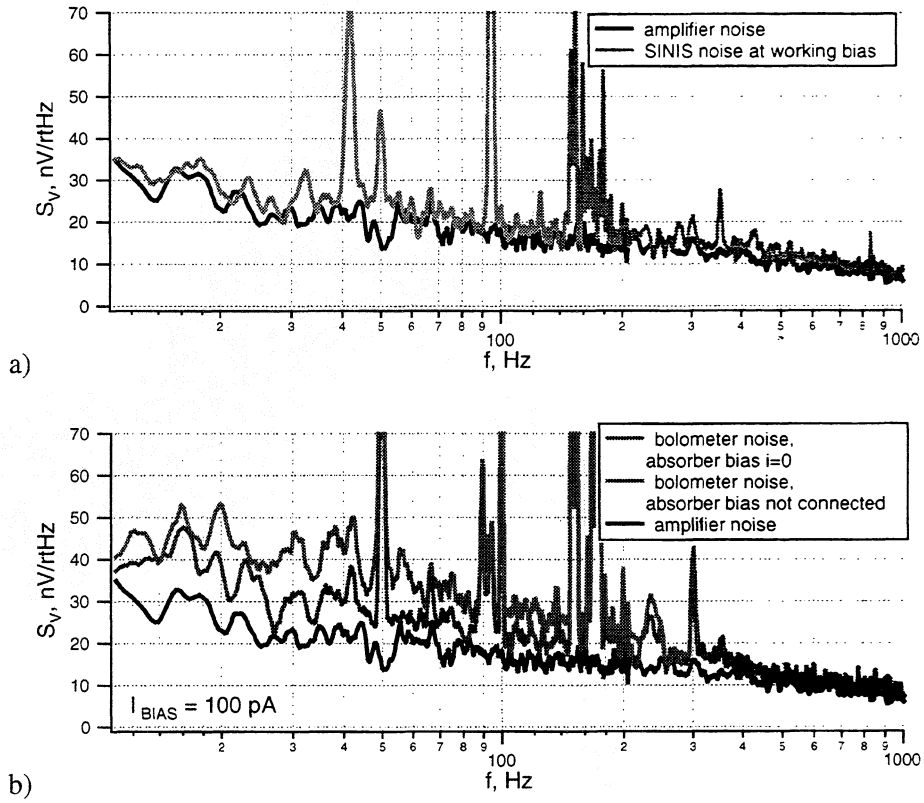

FIG. 7. Noise spectra for a) simple SINIS structure, i.e. without superconducting electrodes connected to the absorber and b) complete microcalorimeter structure equiped with protection NIS junctions and connected to long leads for biasing; the higher noise curve corresponds to leads terminated by a current source. The lowest curve in the both graphs is the amplifier noise.

Disregarding the input noise, the performance of the detector will be limited by thermal fluctuations in the absorber and the noise introduced by the electron temperature readout. The level of thermal fluctuations at a given operating temperature depends on dimensions and material of the absorber. Those, however, can not be varied freely – the absorber length is restricted to a value needed to provide proper impedance for match to the antenna and its width and thickness can not be reduced below certain technological limits. Also, the material choice is bound to the fabrication technology.

On the other hand, the noise from the read-out is a function of many parameters (tunnel junction resistance, number of the junctions, working point, amplifier performance etc.), which can be readily adjusted. Moreover, the noise contribution from the read-out will dominate in all practical configurations. That gives a motivation for optimizing the read-out parameters, and in the following section we will discuss what calculations can aid this process.

4. Optimizing the readout performance

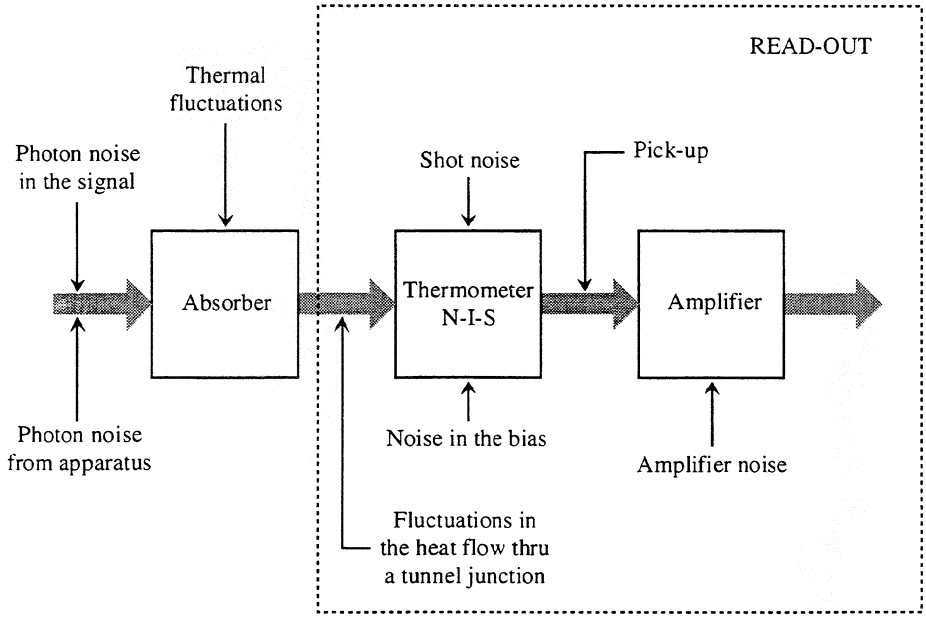

FIG. 8. Scheme of different noise contributions in the NHEB.

Different noise contributions adding to the useful input signal are depicted in fig. 8. The noise equivalent power of the detector can be expressed as

$$NEP^2 = NEP_{IN}^2 + 4k_B T^2 (G - G_{IJ}) + S_J(0) + \frac{S_I^{bias}(0)\left|\frac{dV}{dI}\right|_I^2 + 2eI\left|\frac{dV}{dI}\right|_I^2 + S_V^{ampl}(0) + S_V^{pick-up}(0)}{\left|dV/dT\right|_I^2} G^2$$

where

NEP_{IN}^2 is the photon and other noise coming with the signal to the input,

$4k_B T^2 (G - G_{TJ})$ – noise from thermal fluctuations in the absorber. (G-G_{TJ}) is the thermal conductance from the electron gas in the absorber to the lattice and environment. The thermal conductance due to the tunnel junctions is excluded here, since it is incorporated in the next term,

$S_P(0)$ – "heat flow noise", a component similar to shot noise, but related to the transfer of energy by quasi-particles tunneling through the junction.

$2eI \coth(eV/2T) \approx 2eI$ – current fluctuations due to discreteness of charge (shot noise)

$S_I^{bias}(0)$ – current fluctuations in the external bias applied to the junction

$S_V^{ampl}(0)$ – voltage noise of the amplifier (we assume a high-impedance FET-amplifier)

$S_V^{pick-up}(0)$ – voltage induced in the leads going from the sample to the amplifier (microphonics and rf-field detection)

$|dV/dT|_I$ – temperature responsivity of an NIS-junction at the working bias, and

G – total thermal conductance from the electron gas in the absorber to its environment.

One term here is "new" in the sense that it, to our knowledge, has not been included in any similar analysis before, and this is $S_P(0)$ [6]. If a voltage less then Δ/e is applied over an NIS junction, there will be an energy flow from the normal metal to the superconductor. The effect can be used to cool the normal metal [5] and, accordingly, this energy flow is often called "cooling power":

$$P(V,T_N,T_S) = \frac{1}{e^2 R_N} \int_{-\infty}^{+\infty} d\varepsilon \frac{\theta(\varepsilon^2 - \Delta^2(T_S))|\varepsilon|}{\sqrt{\varepsilon^2 - \Delta^2(T_S)}} (\varepsilon - eV)[f_N(\varepsilon - eV) - f_S(\varepsilon)],$$

where T_N and T_S are temperatures of the normal and superconducting electrodes, $\Delta(T_S)$ is the gap in the superconductor, f_N and f_S are electron distributions in respective electrodes. This expression is very similar to the expression is very for current going through an NIS junction

$$I(V,T_N) = \frac{1}{eR_N} \int_{-\infty}^{+\infty} d\varepsilon \frac{\theta(\varepsilon^2 - \Delta^2(T_S))|\varepsilon|}{\sqrt{\varepsilon^2 - \Delta^2(T_S)}} [f_N(\varepsilon - eV) - f_S(\varepsilon)],$$

but here every tunneling event results in transferring a portion of energy (ε-eV). Since the tunneling events are random and independent, there will be a heat flow noise similar to the usual shot noise. Calculating its spectral density is, however, somewhat more complicated, since the portions of energy are not all the same. The way to do this is to

integrate contributions $dS_{P,\varepsilon} = 2(\varepsilon - eV)\coth(eV/2T)P_e d\varepsilon$ from electrons with a particular energy in the range (ε, ε+dε) over all possible energies:

$$S_P(0) = \frac{2}{e^2 R_N} \coth\frac{eV}{2T} \int_{-\infty}^{+\infty} d\varepsilon \frac{\theta(\varepsilon^2 - \Delta^2(T_S))|\varepsilon|}{\sqrt{\varepsilon^2 - \Delta^2(T_S)}} (\varepsilon - eV)^2 [f_N(\varepsilon - eV) - f_S(\varepsilon)] .$$

The heat flow noise is growing with applied voltage, respectively applied current, thus affecting the upper limit of the optimal range of the bias current for the temperature reading.

From the expression for the total noise one can see that the individual contributions from the different noise sources depend on the absorber properties (G), the shape of the NIS junction's IV-curve (dV/dI, dV/dT), and the working point $I=I_{bias}$. It is also worth to notice that in the theoretical calculations the temperature responsivity dV/dT as a function of bias current I can have a logarithmic singularity at $I \to 0$ (be arbitrary large). This may be misleading (suggesting very low bias currents), because this singularity does not exist in nature, being destroyed by fluctuations near $I=0$.

We can use a computer program to simulate the total noise for any given set of parameters. For the integral giving the IV-characteristics of an NIS junction there is a good analytical approximation, which is suitable for fast calculations. But this is not the case for the heat flow integral, and its computing in every point slows down the model a lot. Fortunately we can separate the tasks. Sets of noise data can be pre-compiled for a specific working temperature T, superconductor with energy gap Δ, and tunnel junction quality in terms of sub-gap conductance $r_o = R(0)/R_N$. Then we can combine those half-ready arrays by substituting all the other parameters of the device:

absorber size and material $\Sigma\Omega$,
current bias source with noise $S_{I.bias}(0)$,
amplifier with noise $S_{ampl}(0)$,
input noise NEP_{IN},
normal resistance of tunnel junctions R_N, and
working bias current I_{bias}.

This can be done really fast, and we have actually made a computer program where one can gradually tune any of those parameters and see on a screen in real time how it affects every noise component and the total NEP. Examples of how the different noise components and the total NEP depend on the SINIS bias current are given in fig. 9 for two different values of R_N and two different temperatures.

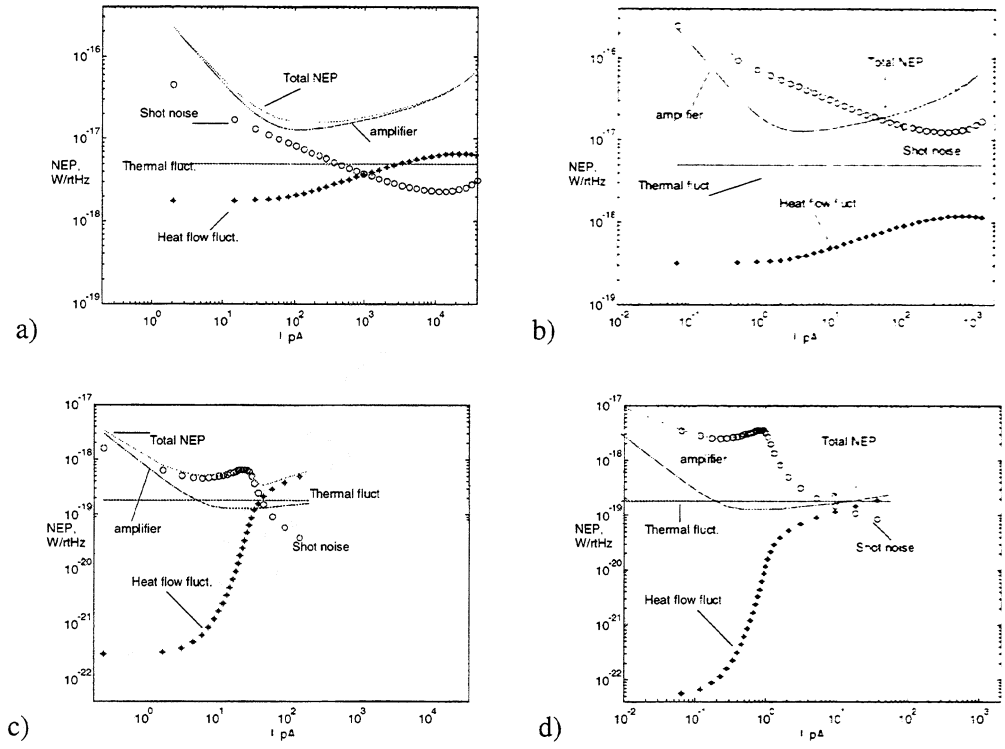

FIG. 9. Different noise components and the total noise calculated as function of SINIS bias current for R_N=1 kΩ (a,c) and R_N = 30 kΩ (b,d) /R_N per one junction/ assuming working temperature of T=300 mK (a,b) and T=100 mK (c,d).

5. Conclusion

We have managed to demonstrate a reasonable performance of the microcalorimeter which we aim to use as power sensor in an integrated antenna-coupled bolometer. We could do this also at temperatures below 100 mK, where the responsivity of the sensor is much higher than in our earlier results (for 300 mK). The measured noise level corresponds to about NEP = $5 \cdot 10^{-18}$ W/Hz$^{1/2}$, and it is dominated by the input noise external to the sensor itself and the amplifier noise. Some refinement of the experiment is still needed to make a fully calibrated characterization of the device.

We considered the noise components determining the practical performance of the future detector, some of them not referred to in earlier analyses of the similar kind. In particular, we payed attention to the heat flow noise, important at higher thermometer bias currents. We also showed how noise optimization can be performed in a model, co-adjusting two or several device and operation parameters at the same time.

References

[1] P.L. Richards, J. Appl. Phys. **76** (1), 1 (1994).

[2] A.T. Lee, S-F. Lee, J.M. Gildemeister, and P.L. Richards, Proc. of the 7th Int. workshop on Low Temperature Detectors, Munich, July-Aug 1997, pp 123-125.

[3] M. Nahum, P.L. Richards, and C.A. Mears, IEEE Trans. Appl. Supercond. **3**, 2124 (1993).

[4] M. Nahum and J. Martinis, Appl. Phys. Lett. **63**(22), 3075 (1993).

[6] M.M. Leivo, J.P. Pekola, and D.V. Averin, Appl. Phys. Lett., **68** (14), 1996 (1996).

[5] L.S. Kuzmin, D.S. Golubev, and M. Willander, *SIN tunnel junction as a temperature sensor*, draft.